Journal of Fluorine Chemistry 241 (2021) 109677

Contents lists available at ScienceDirect

Journal of Fluorine Chemistry

journal homepage: www.elsevier.com/locate/fluor

Investigation of thermal properties and structure of complex fluoride K_3ZrF_7

Mikhail V. Gorev [a,b,*], Maxim S. Molokeev [a,b], Andrey V. Kartashev [a], Evgeniy I. Pogoreltsev [a,b], Svetlana V. Mel'nikova [a], Natalia M. Laptash [c], Igor N. Flerov [a,b]

[a] Kirensky Institute of Physics, Federal Research Center KSC Siberian Branch, Russian Academy of Sciences, 660036 Krasnoyarsk, Russia
[b] Siberian Federal University, 660074 Krasnoyarsk, Russia
[c] Institute of Chemistry, Far Eastern Department of RAS, 690022 Vladivostok, Russia

ARTICLE INFO

Keywords:
Phase transition
Fluorides
Structure
Heat capacity
Entropy
Thermal expansion

ABSTRACT

X-ray, calorimetric and dilatometric studies of K_3ZrF_7 revealed the existence of the phase transition *Fm*-3*m* ↔ *R*-3*m* at $T_0 = 320$ K. The structural model assumes a disorder of a pentagonal bipyramid ZrF_7 with the following ratio of equivalent orientation positions in the initial and distorted phases: 12 to 6. A good agreement was found between the experimental and model-calculated changes in strain and entropy during the phase transition. A comparative analysis of entropy and structural parameters of related fluorides K_3ZrF_7 - $(NH_4)_2KZrF_7$ - $(NH_4)_3ZrF_7$ was performed. The anomalous behavior of thermodynamic properties in the range 140−230 K is not typical for phase transitions and is accompanied by a significant change in the entropy of the crystal lattice.

1. Introduction

Cubic symmetry is characteristic of many complex fluorine compounds, despite the different coordination of anionic polyhedra, and can very often be lowered by changing external (temperature, hydrostatic or uniaxial pressure) and internal (chemical pressure) parameters [1–8]. As a result, these compounds can undergo single or successive phase transitions, usually of a ferroelastic nature [3–10] and much less often they become antiferromagnets [11–14] or ferroelectrics [15–19].

According to a large number of studies, cubic fluorine compounds with seven-coordinated anionic polyhedra in the form of a pentagonal bipyramid are rather rare [2,20,21], for example, compared with widespread fluorides with six-coordinated anionic units (perovskites, elpasolites, cryolites, etc.) [3,5–10]. Such crystals include, in particular, compounds $A_3Me^{4+}F_7$ (A: NH_4^+, K^+) with Me^{4+}: Hf and Zr as the central atoms of polyhedra [22–25]. An interesting feature of both ammonium-containing complex fluorides is the large number of successive structural transformations confirmed by many experimental methods during cooling from the *Fm*-3*m* cubic phase, which is realized near room temperature [26–28]:

Zr – *Fm*-3*m* ($T_0 = 290$ K) ↔ *F*23 ($T_1 = 281$ K) ↔ *Immm* ($T_2 = 279$ K) ↔ monoclinic 1 (*I*2/*m*) ($T_3 = 264$ K) ↔? ($T3' = 261$ K) ↔ *P*-1 ($T_4 = 239$ K) ↔ monoclinic 2;

Hf – *Fm*-3*m* ($T_0 = 290$ K) ↔ cubic ($T_1 = 281$ K) ↔ *mmm* (1) ($T_2 = 273$ K) ↔ *mmm* (2) ($T_3 = 266$ K) ↔ *mmm* (3) ($T_4 = 259$ K) ↔? ($T_5 = 231$ K) ↔ 2/*c* ($T_6 = 229$ K) ↔? .

It is seen that the substitution of the central atom is accompanied by a small change in the number of phase transitions in almost the same temperature ranges, but a significant change in the symmetry of some low temperature phases. The total entropy changes associated with the sequence of structural transformations are rather large in both compounds and close to each other: $\Sigma\Delta S_i = 14.5$ J/mol K (Zr) and $\Sigma\Delta S_i = 10.6$ J/mol K (Hf). However, the relatively small entropies of individual transformations [26,27] cannot be considered as related to some order-disorder processes which contradicts structural models [22–24,28–30].

Recently, we performed a study of zirconium fluoride with a partial substitution of the ammonium group with a monoatomic potassium cation in the ratio 2 : 1, which revealed, on the one hand, the preservation of the *Fm*-3*m* cubic symmetry in $(NH_4)_2KZrF_7$ and, on the other hand, a significantly different picture of structural transformations *Fm*-3*m* ($T_0 = 333$ K) ↔ $P4_2/ncm$ ($T_1 = 329$ K) ↔$P4_2/nmc$ and a strong decrease in the total entropy associated with successive structural distortions, $\Sigma\Delta S_i = 8$ J/mol K [31,32]. Taking into account the closeness of the ionic radii of the monovalent NH_4^+ and K^+ cations, it could be assumed that the main reason for the observed phenomena may be

* Corresponding author at: Kirensky Institute of Physics, Federal Research Center KSC Siberian Branch, Russian Academy of Sciences, 660036 Krasnoyarsk, Russia.
E-mail address: gorev@iph.krasn.ru (M.V. Gorev).

https://doi.org/10.1016/j.jfluchem.2020.109677
Received 23 September 2020; Received in revised form 30 October 2020; Accepted 30 October 2020
Available online 2 November 2020

related to the possibility of occupation of nonequivalent crystallographic positions (8*c* and 4*b*) by both species. X-ray examination confirmed this hypothesis: indeed, the chemical formula of the synthesized compound was $[(NH_4)_{0.672}K_{0.328}]_2[(NH_4)_{0.732}K_{0.268}]ZrF_7$ or in summary $(NH_4)_{2.08}K_{0.92}ZrF_7$. Nevertheless, it is obvious that the ammonium group plays a significant role in the formation of the degree of disordering the initial cubic phase.

In this regard, it is of absolute interest to compare the above data with the picture of phase transitions in crystals with monatomic cations in both positions 4*b* and 8*c*. However, the available information about structure and phase transitions in K_3ZrF_7 as well as K_3HfF_7 is contradictory [21–24,33,34]. X-ray studies showed that at room temperature, the cubic structure of K_3ZrF_7 (sp. gr *Fm*–3*m*) is equivalent to that in $(NH_4)_3ZrF_7$ and was characterized by a strong disordering of ZrF_7^{3-} anionic polyhedra, which were supposed to have sixteen equivalent orientations [22]. The first NMR studies of potassium-containing fluoride revealed an isotropic reorientation of ZrF_7^{3-} at room temperature and the existence of a phase transition from cubic to orthorhombic phase between 254 and 224 K [33,34]. The results of subsequent detailed NMR studies confirmed a significant degree of disordering of anionic polyhedra. At the same time, they showed that the low-temperature orthorhombic structure remains disordered, but as a result of the phase transition at 265 K, the number of possible orientations of the pentagonal bipyramid decreases to four [23].

In comparison with the above results, the study of differential-time perturbation-angle correlation revealed very interesting features of phase transitions and low-temperature distorted phases in isostructural fluorides K_3ZrF_7 and K_3HfF_7 [24]. Two phase transitions were detected in hafnium compound with the following symmetry change during heating: orthorhombic ↔ tetragonal ↔ cubic. The first of the structural transformations occurred at 275 K. The exact temperature of the transition to the cubic phase was not determined, and the authors [24] only stated that this transformation occurs gradually in a wide temperature range above room temperature. In this regard, it seems strange that the strong anomalous behavior of some of the parameters, observed in the region of 330 K, as follows from Fig. 3 in [24], was not discussed. Unfortunately, detailed information about phase transitions was provided only for the hafnium complex. However, based on the data of studies of $(NH_4)_3ZrF_7$ and $(NH_4)_3HfF_7$ [26,27], we can confidently assume that in K_3ZrF_7 the transition temperature from the cubic phase may be higher than room temperature. "Ambiguities" similar to those discussed above were often observed when studying phase transitions in complex fluorides using exclusively structural methods. Only thorough comprehensive studies of physical properties and structures can allow us to construct complex *T*-*p* phase diagrams, as was done, for example, for $(NH_4)_3ZrF_7$ [26].

In view of the points considered, further investigation of phase transitions in fluorides with *Fm*-3*m* structure in which the crystallographic positions 4*b* and 8*c* are occupied by the same monatomic cation seemed to be quite justified. In the present paper, we performed detailed investigations of the structure, heat capacity and thermal expansion of K_3ZrF_7.

2. Experimental

Zirconia (ZrO_2) and potassium hydrogen difluoride (KHF_2) of a reagent grade were used for the synthesis of K_3ZrF_7. A significant excess (3–5 fold) of the fluorinating agent is required relative to the stoichiometric reaction:

$$ZrO_2 + 3.5KHF_2 = K_3ZrF_7 + 0.5KOH + 1.5H_2O.$$

The crystals of the complex were obtained by dissolving ZrO_2 in a hot 10–20 % KHF_2 solution. 20 g of KHF_2 were dissolved in 150 mL of distilled water under heating and 2.0 g of ZrO_2 were added to the hot solution with stirring. The solution was quickly filtered. When the solution was cooled, a fine-crystalline precipitate of the complex fell out. Further evaporation of the solution in air led to the formation of octahedral crystals with a size of ≤ 100 μm.

The composition of the complex obtained was checked by chemical analysis using a fluoride ion-selective electrode similar to that for K_2TaF_7 [35]. The content of fluorine was 37.34 % (compared to calculated 38.95 % for K_3ZrF_7). Thus, the real chemical formula of the compound obtained is $K_3Zr(OH)_{0.3}F_{6.7}$. The existence of oxygen in the form of a hydroxide is confirmed by the presence in the infrared spectrum of the complex of a small wide band of stretching vibrations of the OH group at 3200–3500 cm^{-1} and a band in the region of 700–800 cm^{-1}, which is responsible for the strong hydrogen bond of the O–H…F type.

Samples for measuring thermal properties were prepared in the form of quasi-ceramics tablets (d =6 mm, h = 1 mm) by pressing carefully grinded powder.

Structural studies of the K_3ZrF_7 sample were performed by X-ray method using a Bruker D8 ADVANCE powder diffractometer (Cu-Kα radiation). The powder diffraction data for structural analysis were collected at 303 K and 373 K using the Anton Paar heat attachment and linear VANTEC detector. The step size of 2θ was 0.016°, and the counting time was 2 s per step. Additional 25 X-ray patterns were measured from 303 K to 423 K in a narrow 2θ range: 33.2–39.2° (step size 0.016°, 6 s per step) to check for possible symmetry distortion during phase transition accompanied by the appearance of superstructure reflections. The temperature behavior of the cell parameters was studied by measuring 10 patterns from 303 K to 373 K in a wide 2θ range: 5−90° (step size 0.016°, 0.5 s per step).

Structural characterization of the prepared sample was performed at a temperature of 303 K. The results of Rietveld refinement were found to correspond to rhombohedral symmetry (Fig. 1a and Table 1) instead of the tetragonal or cubic symmetry assumed earlier [22–24,34].

The search for phase transitions was carried out in two stages. Preliminary calorimetric measurements were performed on a NETZSCH 204 F1 differential scanning calorimeter (DSC) on a sample weighing 0.06 g. Experiments were carried out in a dry helium stream (20 mL/min) at a heating/cooling rate of 8 K/min.

Exploratory optical studies were performed using an Axioskop-40 polarization microscope and a Linkam LTS 350 temperature chamber in the interval 100–380 K. Due to the small size of octahedral crystals, changes in optical anisotropy were studied only in samples as grown with well-developed opposite faces (111).

Detailed calorimetric studies were carried out in a temperature range of 80−370 K by means of a home-made adiabatic calorimeter with three screens [36]. The mass of the sample was about 0.3 g. Over the whole temperature range investigated, the inaccuracy in the heat capacity determination did not exceed (0.4–0.8) %. The heat capacity of the "sample + heater + contact grease" system was measured using discrete as well as continuous heating. In the former case, the calorimetric step was varied from 1.5 to 3.0 K. In the latter case, the system was heated at rates of $dT/dt \approx 0.15-0.30$ K/min. The heat capacities of the heater and contact grease were determined in individual experiments.

Thermal expansion was measured using a push-rod dilatometer (NETZSCH model DIL-402C) with a fused silica sample holder. The experiments were carried out in a dry He flux in the temperature range of 100−400 K with a heating rate of 3 K/min. To eliminate the influence of thermal expansion of the system, the results were calibrated using quartz as a standard reference. The irreproducibility of the data obtained in successive series of measurements was less than 5 %.

3. Results and discussion

Due to the above-mentioned ambiguity of information about phase transitions in K_3ZrF_7, search calorimetric measurements were performed at the first stage. The results of experiments using DSC with a temperature change rate of ± 8 K/min are shown in Fig. 2. Upon heating, one

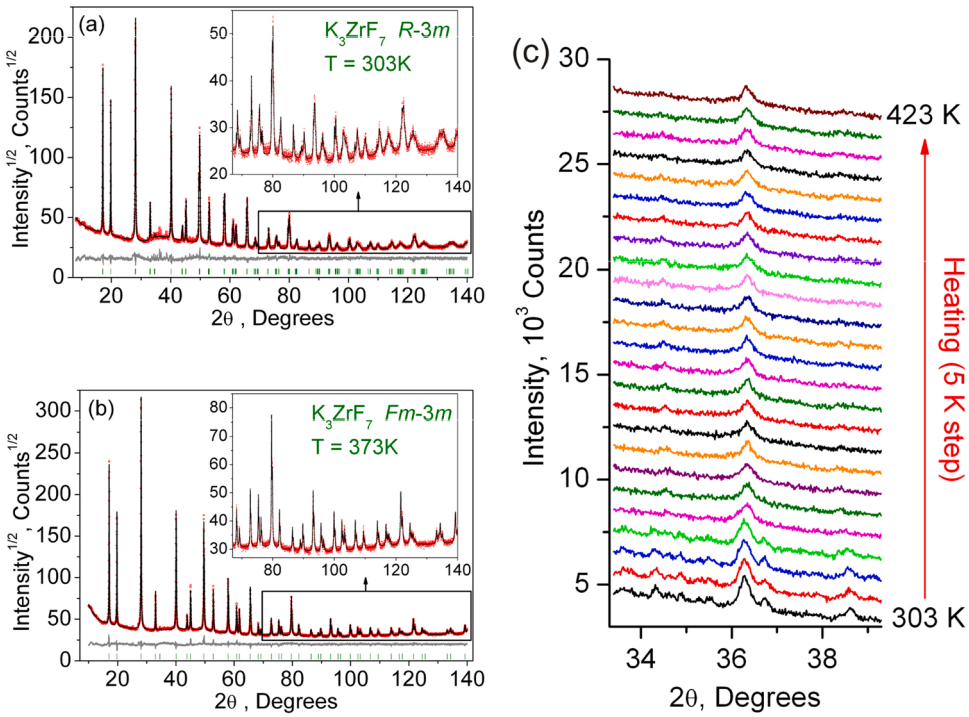

Fig. 1. Difference Rietveld plot of K_3ZrF_7at (a) 303 K (*R*-3*m* phase); (b) 373 K (*Fm*-3*m* phase). (c) Small peaks, which appeared to be superstructure in *R*-3*m* phase, actually are not superstructure but impurity peaks. Their intensities become low and peaks become broad under heating, but they didn't disappear at phase transition point and higher.

Table 1
Main parameters of processing and refinement of the K_3ZrF_7 structure.

T, K	373	303
Sp.Gr.	*Fm*-3*m*	*R*-3*m*
a, Å	9.00080 (7)	6.3355 (1)
c, Å	–	15.6095 (3)
V, Å^3	729.195 (17)	542.60 (2)
Z	4	3
2θ-interval, °	10–140	8–140
R_{wp}, %	5.02	5.81
R_p, %	3.86	4.44
R_{exp}, %	2.43	2.98
χ^2	2.07	1.95
R_B, %	3.29	2.38

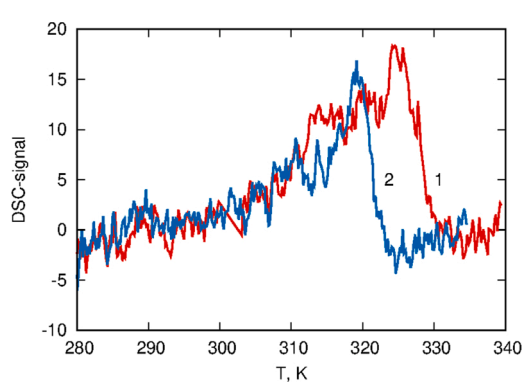

Fig. 2. DSC signal near T_0 during heating (1) and colling (2).

anomaly was detected at 324 K which was shifted upon cooling to 319 K. Such a rather large temperature hysteresis indicates the first order of the phase transition found.

Subsequent detailed experiments using an adiabatic calorimeter

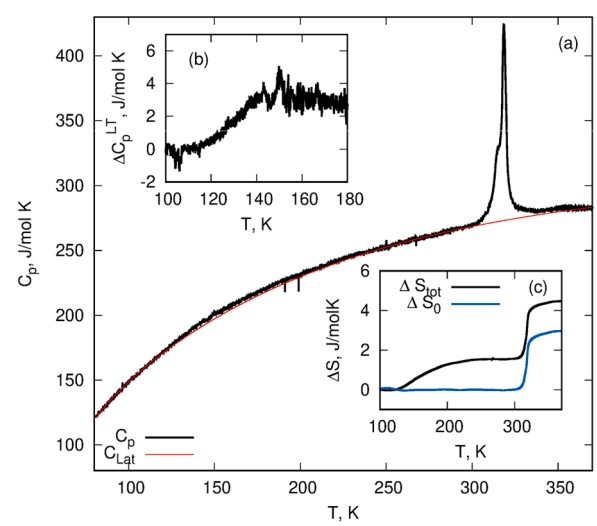

Fig. 3. Temperature dependencies of (a) heat capacity C_p and lattice heat capacity, C_{Lat}, (b) anomalous heat capacity ΔC_p^{LT} at low temperature and (c) anomalous entropies ΔS_{tot} and ΔS_0 of K_3ZrF_7.

showed a slightly different temperature dependence of the heat capacity (Fig. 3). One sharp peak $C_p(T)$ was detected at $T_0 = 320.0 \pm 0.5$ K. In the low - temperature region, an anomalous behavior of heat capacity was detected in a wide temperature range of 140–230 K, which can be considered in two ways. This may be, first, a very blurred peak of C_p, and, second, a stepwise increase in heat capacity, as was observed for $(NH_4)_2KZrF_7$ [32].

Polarizing-optical experiments at room temperature on the $(111)_c$ sample showed the presence of weak bands along $[100]_c$, which disappear on heating in the range 320–325 K and the K_3ZrF_7 crystal becomes optically isotropic. Upon cooling below room temperature, spots of anisotropy of very low intensity appear at about 160 K, which disappear

when heated around 210 K.

X-ray diffraction analysis was also performed at 130 K to check possible changes in symmetry in the low-temperature range. No features were found in the diffraction pattern compared to that at 303 K, except for the displacement of reflection angles in accordance with the decrease in the unit cell parameters (Fig. 4).

The most productive discussion of the mechanism of phase transitions involves a joint analysis of structural and entropic parameters. Information about the latter can be obtained by dividing the total heat capacity, C_p, into lattice, C_{Lat}, and anomalous, ΔC_p, contributions. For this purpose, the procedure for determining the dependence $C_{Lat}(T)$ is performed by fitting experimental data on $C_p(T)$ significantly above and below the phase transition region in the Debye model, followed by C_{Lat} interpolation to the entire temperature region of the measured heat capacity (Fig. 3a).

Fig. 3b shows more clearly the behavior of the anomalous heat capacity in the low-temperature region, ΔC_p^{LT}. The excess heat capacity associated only with the phase transition at T_0, $\Delta C_p^{PT}=C_p\text{-}C_{Lat}$, exists in a narrow temperature range of ~(10–15) K. As a result, despite the rather large value of $\Delta C_p^{PT} = 150$ J/mol K, the corresponding change in entropy was small $\Delta S_0=\int(\Delta C_p^{PT}/T)dT = 3.0 \pm 0.5$ J/mol K (Fig. 3c) and significantly less in comparison with the entropies of successive structural transformations in the related ammonium-containing fluorides $(NH_4)_3ZrF_7$ ($\Sigma\Delta S_i = 14.5$ J/mol K) [26] and $(NH_4)_2KZrF_7$ ($\Sigma\Delta S_i = 8$ J/mol K) [32]. Thus, we can confidently assume that structural distortions in the K_3ZrF_7 cannot be associated with any order-disorder processes during the phase transition.

Fig. 3c also shows the relationship between the total excess entropy, $\Delta S_{tot} = \int(\Delta C_P/T)\,dT$, and the phase transition entropy ΔS_0. The value of $\Delta S_{tot}\text{-}\Delta S_0 = 1.5 \pm 0.3$ J/mol K associated with the step-wise anomaly is many times smaller than the similar parameter for $(NH_4)_2KZrF_7$ (28 ± 3 J/mol K, whose heat capacity shows a similar anomaly in the region of 200 K [32].

It can be assumed that the large difference between the values of ΔS_{tot} - ΔS_0 in potassium and ammonium-potassium fluorides is associated with different changes in the mobility of structural elements when the temperature changes. This assumption is supported by almost identical values C_{Lat} at 100 K and 350 K for K_3ZrF_7 (148 and 270 J/mol·K) and $(NH_4)_2KZrF_7$ (150 and 280 J/mol·K) [32]. In this regard, NMR data for $(NH_4)_2KZrF_7$, which are not currently available, could be very useful for comparison with those for potassium fluoride to reveal the nature of the mobility of ammonium groups.

The results of thermal expansion studies are shown in Fig. 5. Like heat capacity (Fig. 3), volumetric deformation, $\Delta V/V$, and volumetric coefficient of thermal expansion, β, showed anomalous behavior in two temperature ranges. First, at $T_0 = 322.5 \pm 1.0$ K, a rather small positive "jump" in volumetric deformation $\delta V/V \approx 7.5\cdot10^{-4}$ and a large narrow peak $\delta\beta = 50\cdot10^{-6}\,K^{-1}$ are observed, associated with a phase transition. Second, the $\Delta V/V(T)$ and $\beta(T)$ curves show a kink at a temperature of about 140 K and a blurred jump-like increase from ~ $70\cdot10^{-6}$ to ~ $90\cdot10^{-6}$, respectively, over a very wide temperature range of ~140−230 K. The latter anomaly looks like the same in $(NH_4)_2KZrF_7$ observed in the region of 235–270 K [32]. It allows us to assume that the nature of this phenomenon is associated with the ZrF_7 polyhedron.

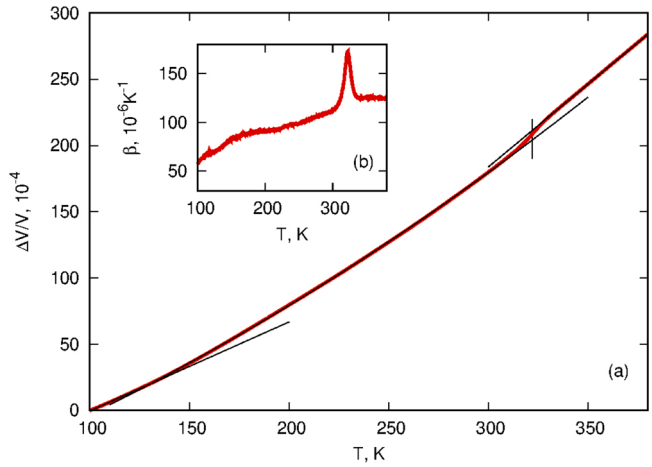

Fig. 5. Temperature dependencies of (a) strain and (b) the thermal expansion coefficient of K_3ZrF_7.

The results of structural characterization of the sample under study at 303 K and 130 K presented in Fig. 4 did not show any differences in the X-ray diffraction patterns, except for changes in the unit cell parameters.

Here we will consider the behavior of structural parameters in a wide temperature change including the phase transition region. Almost all peaks of the powder pattern at 373 K (Fig. 1b), except for small peaks of impurities, were indexed by a cubic cell (*Fm-3m*) with parameters close to those previously reported for $(NH_4)_2KZrF_7$ [31]. However, this model was not selected for refinement, since it was not possible to find the perfect ZrF_7 polyhedron from the disordered model. Therefore, first of all, an ideal pentagonal ZrF_7 bipyramid with local *mm*2 symmetry was constructed as a rigid body (Fig. 6).

Crystal structure was solved in TOPAS 4.2 [37] using a simulated annealing procedure applied to randomized three orientation angles of ZrF_7 polyhedron. The best model with the lowest *R*-factors showed that the local planes of symmetry *m* of the bipyramid almost coincide with the planes of symmetry *m* of the crystal structure.

The angles of deviation of the equatorial and polar local *m* planes from the ideal *m* planes of the crystal structure were 11.9° and 9.5°, respectively. Therefore, it was decided to orient the pentagonal bipyramid manually in order to superpose local *m* planes with the crystal *m* planes. This procedure noticeably simplifies the model, in particular, the three orientation angles of the pentagonal bipyramid were fixed at 0 and only the d_1 and d_2 values were refined. Moreover, to construct bipyramid with a specific orientation, only four independent F^- ions are sufficient

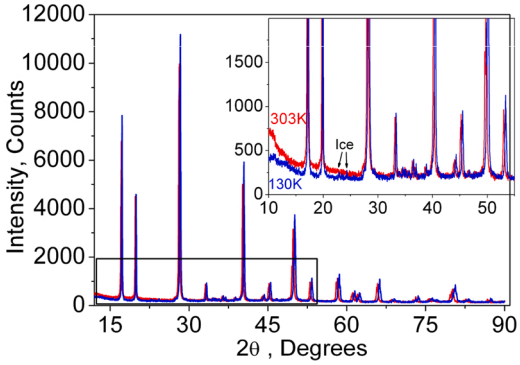

Fig. 4. X-ray powder patterns of K_3ZrF_7 at 303 K and 130 K.

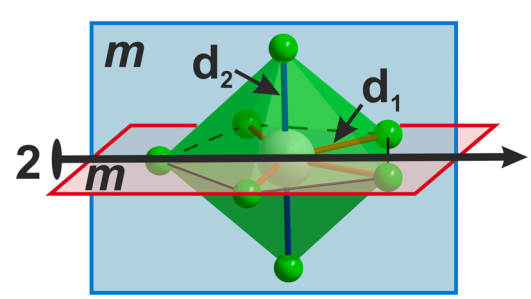

Fig. 6. The ideal ZrF_7 pentagonal bipyramid with local symmetry mm2 was used to solve the crystal structure of K_3ZrF_7 in all phases. Two different bond lengths d(Zr–F) were used in model: d_1 and d_2 for equatorial and polar F ions, respectively.

instead of seven F^- ions in the general orientation. An additional cycle of refinement of the new model was performed, which revealed a good fit (Table 1, Fig. 1b). The crystal structure is depicted in Fig. 7a.

Coordinates of atoms and main bond lengths are in Tables 2 and 3, respectively. The differences between the current model and the model described earlier [22] are as follows: 1) in our model there are four independent F sites instead of three F sites; 2) 12 orientations of ideal pentagonal bipyramids ZrF_7 can be found in our model (Fig. 8a), while it is difficult to find undistorted ZrF_7 polyhedra in the structure proposed earlier [22].

A real splitting of the main strong peaks observed on the X-ray pattern at 303 K indicates a decrease in symmetry. They were indexed in TOPAS 4.2 by trigonal cell (*R*-3*m*) with parameters $a = 6.3317$ Å, $c = 15.5922$ Å and FOM = 45.

Group-theoretical analysis using the internet tool ISODSTORT [38] revealed that the phase transition *Fm*-3*m*↔*R*-3*m* can be described by the emergence of instability at the (0, 0, 0) k_{11}-point (Γ) of the Brillouin zone of a highly symmetric *Fm*-3*m* unit cell (hereinafter, the designation of irreducible representations (irrep) and points of the Brillouin zone are given in accordance with the reference books [39,40]). The Γ_5^+ irrep drives the phase transition, and the transformation can be written as *Fm*-3*m*↔Γ_5^+(η, η, η) ↔*R*-3*m*, where η is the critical order parameter. During the phase transition, the ZrF_7 polyhedron rotates and one K ion moves along the *c* axis, breaking the cubic symmetry.

In this case only one *m* plane of the ZrF_7 pentagonal bipyramid coincides with *m* plane of the crystal structure *R*-3*m* (Fig. 8b, orientation 1), contrary to the cubic phase with a more specific ZrF_7 orientation (Fig. 8a, orientation 1). Therefore, the initial orientation of ZrF_7 in *R*-3*m* has one additional degree of freedom, and the polyhedron can freely rotate around an axis perpendicular to *m* plane mentioned above.

In order to find structure a simulated annealing procedure applied to randomized one orientation angle of ZrF_7 polyhedron was made in TOPAS 4.2. The searching operation quickly converged and led to a model with a global *R*-factor minimum. Checking the crystal structure revealed that the symmetry elements in the *R*-3*m* phase copy the initial orientation into six ZrF_7 another orientations (Fig. 8b). It was found that to construct all orientations of ZrF_7, as was the case in the *Fm*-3*m* phase, only four independent F^- ions are needed. This updated model was used for Rietveld refinement, which appeared to be stable and resulted in low *R*-factors (Table 1). The crystal structure with different orientations of the axes is shown in Fig. 7b and c. Coordinates of atoms and main bond lengths are in Tables 2 and 3, respectively. The temperature dependencies of the cell parameters and the cell volume are presented in Fig. 9a and b, respectively.

The cell parameters showed a strong change in the narrow temperature range near the phase transition point, but the change in the cell volume attributed to the formula unit, $\Delta V/Z$, was small: ~0.1 Å^3, i.e. $\Delta V/V \sim 6 \cdot 10^{-4}$. The latter value is in a good agreement with that found in dilatometric measurements.

Table 2
Fractional atomic coordinates and isotropic displacement parameters (Å^2) of K_3ZrF_7.

	Wyck.	x	y	z	B_{iso}	Occ.
T = 373 K						
K1	8*c*	1/4	1/4	1/4	4.65 (7)	1
K2	4*b*	1/2	1/2	1/2	4.42 (7)	1
Zr	4*a*	0	0	0	1.62 (6)	1
F1	24*e*	0	0	0.2284 (8)	4.97 (13)	1/6
F2	96*j*	−0.2172 (7)	0	0.0706 (2)	4.97 (13)	1/12
F3	96*j*	−0.1342 (5)	0	−0.1848 (6)	4.97 (13)	1/12
F4	24*e*	0	0.2073 (12)	0	4.97 (13)	1/3
T = 303 K						
K1	6*c*	0	0	0.25041 (19)	3.81 (3)	1
K2	3*b*	0	0	0.5	4.22 (5)	1
Zr	3*a*	0	0	0	1.269 (14)	1
F1	18*h*	−0.0893 (6)	2*x*	0.1182 (4)	3.24 (11)	1/6
F2	36*i*	−0.3412 (11)	−0.0552 (4)	0.03653 (13)	3.24 (11)	1/6
F3	36*i*	−0.1216 (6)	0.1444 (10)	−0.0956 (3)	3.24 (11)	1/6
F4	18*h*	0.1567 (8)	2*x*	0.0585 (5)	3.24 (11)	1/3

Table 3
Main bond lengths (Å) of K_3ZrF_7.

T = 373 K			
K1—F2^{i}	2.785 (5)	Zr—F1	2.056 (6)
K1—F3^{ii}	2.548 (5)	Zr—F2	2.056 (6)
K2—F1^{iii}	2.445 (7)	Zr—F3	2.056 (6)
K2—F2^{iv}	2.624 (6)	Zr—F4	1.866 (11)
K2—F4^{v}	2.635 (11)		
T = 303 K			
K1—F1	2.284 (7)	Zr—F1	2.089 (6)
K1—F2^{i}	2.542 (6)	Zr—F2	2.089 (6)
K2—F3^{i}	2.463 (5)	Zr—F3	2.089 (5)
K2—F4^{ii}	2.570 (9)	Zr—F4	1.947 (9)

Symmetry codes:
Fm-3*m* phase: (i) -*x*, -*y*, *z*; (ii) -*x*, *y*, -*z*; (iii) *z*, *y*+1/2, -*x*+1/2; (iv) *x*+1, *y*+1/2, *z*+1/2; (v) -*y*+1, *x*+1/2, *z*+1/2.
R-3*m* phase: (i) -*x*-1/3, -*y*+1/3, -*z*+1/3; (ii) *x*-1/3, *y*-2/3, *z*+1/3.

The results of the present study we will discuss considering the effect of the cationic and central atom substitution on the phase transitions in the series of related complex fluorides A_3MeF_7 (A: $(NH_4)_3$, K; Me: Zr, Hf) characterized by a cubic symmetry in the initial phase (sp. gr. *Fm*-3*m*, *Z* = 4) [22,24,30,31]. A sharp decrease in the number of phase transitions as the concentration of potassium in complex zirconates and

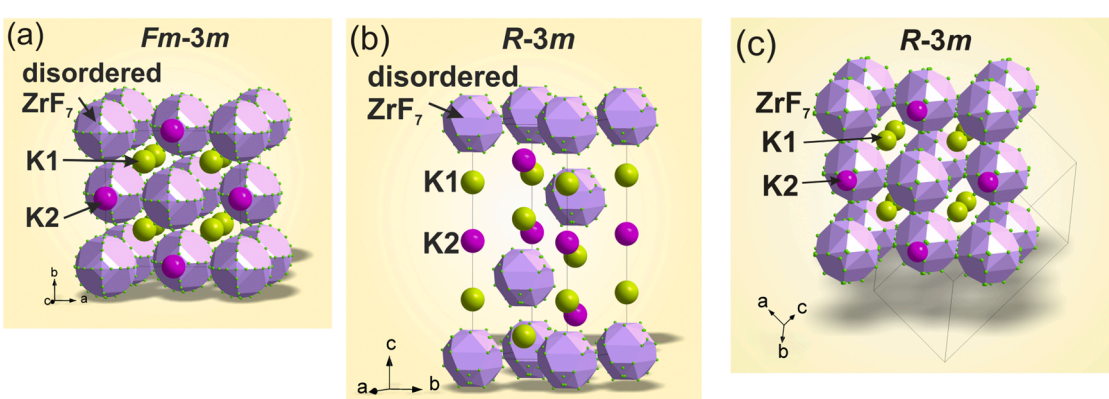

Fig. 7. Crystal structure of K_3ZrF_7: (a) *Fm*-3*m* at 373 K; b) *R*-3*m* at 303 K, c) *R*-3*m* at 303 K with cubic-like structure.

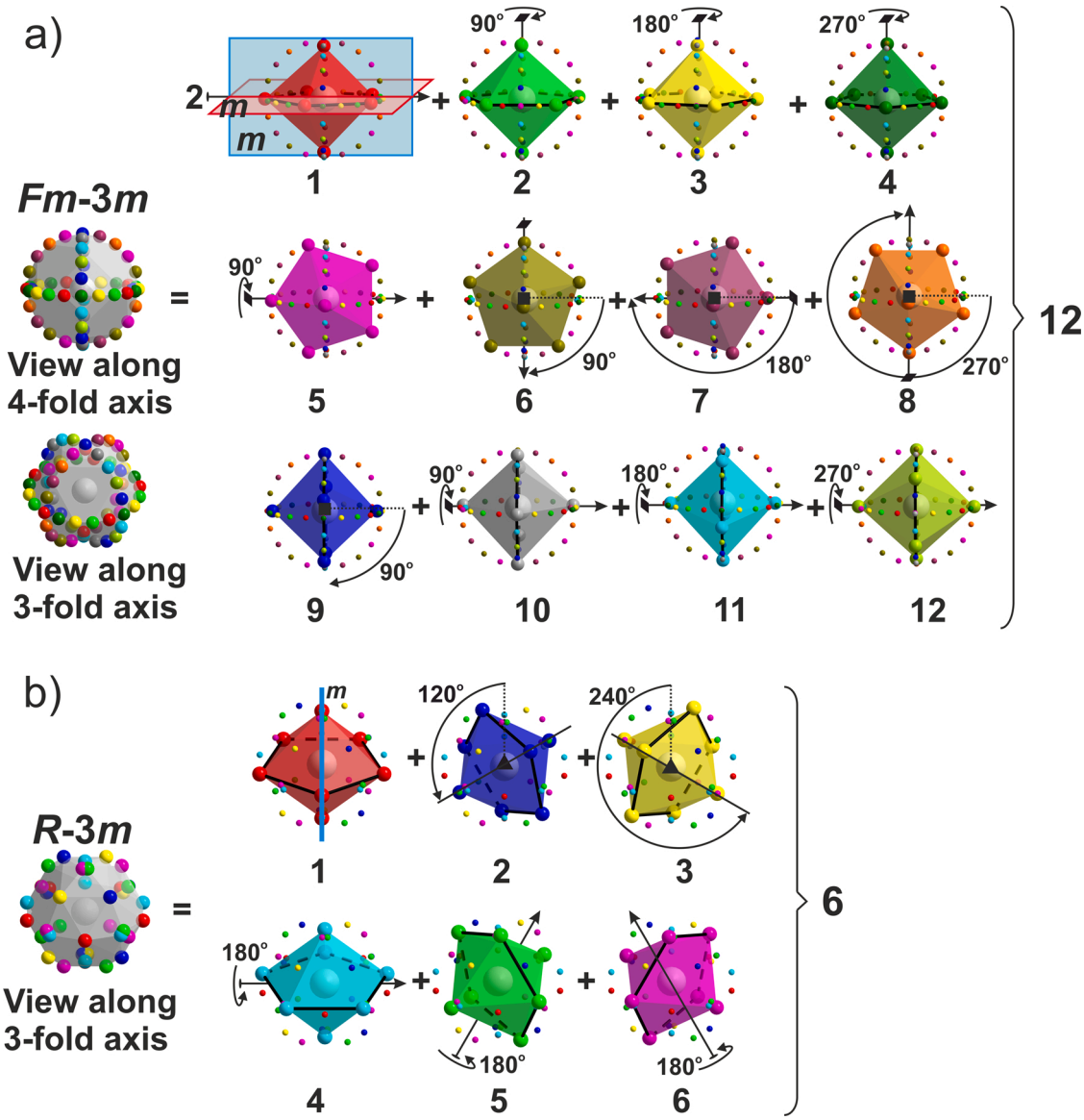

Fig. 8. Separation of complex disordered ZrF_n polyhedron into particular orientations of ideal pentagonal bipyramids ZrF_7: a) in Fm-3 m phase; b) in R-3 m phase. The twelve orientations of ZrF_7 in Fm-3 m phase can be obtained by applying symmetry elements: a1) Initial orientation of ZrF_7 in Fm-3 m phase, the ZrF_7 goes through two m planes of crystal; a2) Rotation around 4-fold axis along b at 90°; a3) Rotation around 4-fold axis along b at 180°; a4) Rotation around 4-fold axis along b at 270°; a5) Rotation around 4-fold axis along a at 90°; a6) Rotation around 4-fold axis along a at 90° and after that along b at 90°; a7) Rotation around 4-fold axis along a at 90° and after that along b at 180°; a8) Rotation around 4-fold axis along a at 90° and after that along b at 270°; a9) Rotation around 4-fold axis along c at 90°; a10) Rotation around 4-fold axis along c at 90° and after that along a at 90°; a11) Rotation around 4-fold axis along c at 90° and after that along a at 180°; a10) Rotation around 4-fold axis along c at 90° and after that along a at 270°. The six orientations ZrF_7 in R-3 m phase can be obtained by applying symmetry elements: b1) Initial orientation of ZrF_7 in R-3 m phase, the ZrF_7 goes through m plane of crystal; b2) Rotation around 3-fold axis at 120°; b3) Rotation around 3-fold axis at 240°; b4) Rotation around twofold axis along a; b5) Rotation around twofold axis along b; b6) Rotation around twofold axis along a + b.

hafnates increases suggests that the ammonium cation certainly plays a significant role in the formation of stable crystalline phases.

Recently, the structure of the *Fm*-3*m* phase in some of these compounds, $(NH_4)_3ZrF_7$, $(NH_4)_3HfF_7$ and $(NH_4)_2KZrF_7$, was suggested to be strongly disordered [29–31]. Similar to K_3ZrF_7, to preserve the cubic symmetry of the crystal lattice, a pentagonal bipyramid ZrF_7 with *mm*2 local symmetry was considered as a rigid body, which must be orientationally disordered in at least 12 equal positions. In addition, in zirconium and hafnium fluorides, the ammonium groups were also assumed to be disordered, having four (site 8*c*) and eight (site 4*b*) spatial orientations. Despite the lack of a refinement of the structure for $(NH_4)_2KZrF_7$, it is highly likely that in the ideal *Fm*-3*m* structure two ammonium ions in position 8*c* are also disordered while the spherical potassium cation in position 4*b* is ordered. In K_3ZrF_7, cations K^+ are ordered occupying both, 8*c* and 4*b*, positions.

Thus, a sequential replacement of the tetrahedral ammonium ion with a spherical potassium one is accompanied by decrease in structural disorder and, as a result, should lead to a decrease in the entropies of the phase transitions, $\Sigma\Delta S_i$, which in the case of the total ordering of structural elements are: $(NH_4)_3ZrF_7$ - $2R\ln 4 + R\ln 8 + R\ln 12 \approx 61$ J/mol·K; $(NH_4)_2KZrF_7$ - $2R\ln 4 + R\ln 12 \approx 44$ J/mol·K; K_3ZrF_7 - $R\ln 12 \approx 21$ J/mol·K. This tendency was supported by the experimental values of $\Sigma\Delta S_i$ (J/mol·K): $(NH_4)_3ZrF_7$ - 14.5 [26], $(NH_4)_2KZrF_7$ - 8 [32], K_3ZrF_7 - 3, which, however, were found significantly less in comparison with suggested from the structural models total disorder – total order. Of course, the analysis must take into account some additional experimental features.

The observed sequential decrease in the total entropy of phase

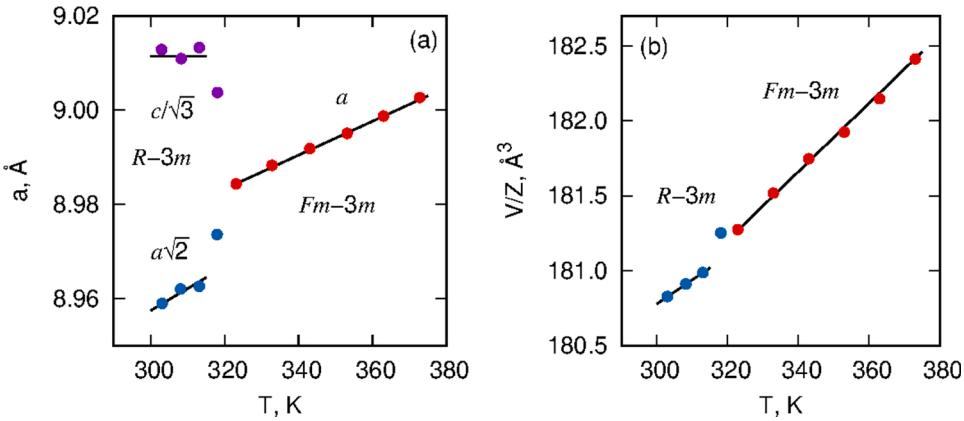

Fig. 9. Temperature behavior of (a) cell parameters for Fm-3 m and R-3 m phases and (b) formula cell volume V/Z for Fm-3 m and for R-3 m phases.

transitions during K → NH_4 substitution is consistent with an increase in the symmetry of the low-temperature phase of the fluorides under consideration (monoclinic in $(NH_4)_3ZrF_7$; tetragonal in $(NH_4)_2KZrF_7$; rhombohedral in K_3ZrF_7), which indicates one mechanism of structure distortion.

Since the lowest temperature in calorimetric experiments was about 100 K, one could assumed that compounds considered exhibit additional phase transitions at more lower temperature. However, at least in the case of $NH_4)_3ZrF_7$, the Raman study did not reveal any peculiarities in the spectra of the low temperature phase down to 7 K [28].

In accordance with the X-ray study, the nonequivalent crystallographic positions 4*b* and 8*c* in the crystal lattice of $(NH_4)_2KZrF_7$ are occupied by both K^+ and NH_4^+ ions due to a very small difference in their ionic radii. Taking into account the refined occupancies and linear restriction occ(NH_4)+occ(K) = 1 for both sites [31] leads even to increase in entropy $\Delta S = R(\ln 12 + 1.35\ln 4 + 0.732\ln 8) \approx 49$ J/mol K.

In the rhombohedral phase of K_3ZrF_7 the pentagonal bipyramid ZrF_7 remains partially disordered occupying 6 positions compared to 12 in a cubic phase and entropy of the phase transition should be only $\Delta S = R\ln 2 = 5.76$ J/mol·K. However, even this relatively small value remains greater than the experimental magnitude of ΔS_0.

It should be noted that a significant difference in the entropies determined experimentally and within the framework of the models of the disordered structure *Fm*-3*m* was also observed for compounds with six-coordinated anionic octahedra A_3MeF_6 [5–9]. From our point of view, the reason for this very strange circumstance may well be related to the fact that the maximum possible disorder in the initial phase *Fm*-3*m* is considered when constructing the model. However, actually the cubic symmetry in both A_3MeF_6 and A_3MeF_7 can be preserved due to strong anharmonic vibrations of critical ions when the time of ion hopping between equivalent positions is comparable and even longer than the time spent in them. In this case, the entropy of the phase transition will be significantly less than the entropy associated with order-disorder processes [41,42].

This hypothesis is confirmed by the results of studies of the elpasolite $Cs_2NaNdCl_6$ and perovskite $KMnF_3$ (*Pm*-3*m*, $Z = 1$), which at the first stage were also assumed to be disordered in the initial phases, despite the very low entropy of phase transitions, $\Delta S \leq 0.2R$ [3,42]. However, the refinement of the same structures within the framework of unsaturated anharmonicity of the vibrations of critical atoms made it possible to conclude that it is very difficult to choose the appropriate model in view of the very close values of the *R*-factor [43,44]. Thus, in controversial cases, the value of the entropy change can be considered as a reference point when choosing a model of at least the initial phase structure [42].

As for anomalies on the dependencies $C_p(T)$, $\Delta V/V$(T) and $\beta(T)$ in the low-temperature phase of K_3ZrF_7 (Figs. 3 and 4), it is currently difficult to imagine the reasons for such a strange behavior. However, the absence of differences in the X-ray patterns at 303 and 130 K shows that there are no symmetry changes associated with the phase transition. It should be noted that similar behavior of heat capacity and thermal expansion was also observed in $(NH_4)_2KZrF_7$ [32]. In this situation, NMR data can be very useful since it cannot be ruled out that the discussed low-temperature anomalies are associated with a change in the mobility of ionic groups. Indeed, in accordance with [23,34], the ZrF_7^{3-} ions in K_3ZrF_7 were stationary on the NMR timescale below ~120 K and then they reoriented isotropically above ~230 K. In the intermediate region, 120 < *T* < 230 K, the ^{19}F second moment as a function of temperature, $M_2(T)$, exhibits a strong change from 0.6 to 0.9 G^2 [23]. The large difference between the values of ΔS_{tot} - $\Sigma\Delta S_i$ for $(NH_4)_2KZrF_7$ [32] and K_3ZrF_7 (Fig. 3c) can also be considered as related to a possible change in the mobility of structural elements depending on the composition of the compound.

4. Conclusions

A detailed study of the heat capacity, thermal expansion and structure of complex K_3ZrF_7fluoride performed over a wide temperature range revealed a first order phase transition *Fm*-3*m* ↔ *R*-3*m* at $T_0 = 320$ K. The experimental magnitudes of change in the volume strain and entropy associated with the structural transformation were quite small: $\Delta(\Delta V/V) = 7.5 \cdot 10^{-4}$ and $\Delta S_0 = 3$ J/mol K.

Careful structural analysis has shown that the phase transition is accompanied by rotation of the pentagonal bipyramid ZrF_7^{3-} and displacement of the potassium ion. It is assumed that both phases are disordered with a ratio of equivalent orientations of 12 (*Fm*-3*m*) to 6 (*R*-3*m*), which should lead to the entropy change, $\Delta S_0 = 5.8$ J/mol K close to the experimental value. The change in the volumetric deformation, referred to one formula unit, $\Delta(\Delta V/Z) \approx 6 \cdot 10^{-4}$ Å^3, is in good agreement the data of dilatometric measurements.

The role of the chemical pressure determined by cationic substitution in the formation of the structural order/disorder of the initial and distorted phases in a series of related fluorides $(NH_4)_3ZrF_7$ - $(NH_4)_2KZrF_7$ - K_3ZrF_7 was elucidated by comparative analysis of entropy and structural parameters.

An additional anomaly, blurred over a very wide temperature range of 140–230 K, was observed in calorimetric, dilatometric, and polarizing-optical experiments on K_3ZrF_7, similar to that detected in related compound $(NH_4)_2KZrF_7$ [32]. Taking into account the NMR data [23,34] and the absence of changes in the structure, it can be assumed that low-temperature anomalies in both compounds are associated with changes in the mobility of the pentagonal bipyramid ZrF_7^{3-}.

Declaration of Competing Interest

The authors report no declarations of interest.

Acknowledgements

The reported study was funded by RFBR according to the research project No. 18-02-00269 a. X-ray and dilatometric data were obtained using the equipment of Krasnoyarsk Regional Center of Research Equipment of Federal Research Center "Krasnoyarsk Science Center SB RAS".

References

[1] Z. Mazej, R. Hagiwara, Hexafluoro-, heptafluoro-, and octafluoro-salts, and $[M_nF_{5n+1}]^-$ (n = 2, 3, 4) polyfluorometallates of singly charged metal cations, Li^+ - Cs^+, Cu^+, Ag^+, In^+ and Tl^+, J. Fluorine Chem. 128 (2007) 423–437, https://doi.org/10.1016/j.jfluchem.2006.10.007.

[2] A. Tressaud (Ed.), Functionalized Inorganic Fluorides: Synthesis, Characterization and Properties of Nanostructured Solids, Wiley-Blackwell, 2010, https://doi.org/10.1002/9780470660768.

[3] I.N. Flerov, M.V. Gorev, K.S. Aleksandrov, A. Tressaud, J. Grannec, M. Couzi, Phase transitions in elpasolites (ordered perovskites), Mater. Sci. Eng. 24 (1998) 81–151, https://doi.org/10.1016/S0927-796X(98)00015-1.

[4] M. Leblanc, V. Maisonneuve, A. Tressaud, Crystal chemistry and selected physical properties of inorganic fluorides and oxide-fluorides, Chem. Rev. 115 (2015) 1191–1254, https://doi.org/10.1021/cr500173c.

[5] I. Flerov, M. Gorev, M. Molokeev, N. Laptash, Ferroelastic and ferroelectric phase transitions in fluoro- and oxyfluorometallates, in: A. Tressaud, K. Poeppelmeier (Eds.), Photonic and Electronic Properties of Fluoride Materials, Elsevier, Boston, 2016, pp. 355–381, https://doi.org/10.1016/B978-0-12-801639-8.00016-7.

[6] M.V. Gorev, I.N. Flerov, A. Tressaud, Thermodynamic properties and p-T phase diagrams of $(NH_4)_3M^{3+}F_6$ cryolites (M^{3+} : Ga, Sc), J. Phys. Condens. Matter 11 (1999) 7493–7500, https://doi.org/10.1088/0953-8984/11/39/306.

[7] A.A. Udovenko, N.M. Laptash, I.G. Maslennikova, Orientation disorder in ammonium elpasolites. Crystal structures of $(NH_4)_3AlF_6$, $(NH_4)_3TiOF_5$ and $(NH_4)_3FeF_6$, J. Fluorine Chem. 124 (2003) 5–15, https://doi.org/10.1016/S0022-1139(03)00166-0.

[8] I. Flerov, M. Gorev, J. Grannec, A. Tressaud, Role of metal fluoride octahedra in the mechanism of phase transitions in A_2BMF_6 elpasolites, J. Fluorine Chem. 116 (2002) 9–14, https://doi.org/10.1016/S0022-1139(02)00068-4.

[9] I.N. Flerov, M.V. Gorev, K.S. Aleksandrov, A. Tressaud, V.D. Fokina, Ferroelastic phase transitions in fluorides with cryolite and elpasolite structures, Crystallogr. Rep. 49 (2004) 100–107, https://doi.org/10.1134/1.1643969.

[10] J. Lin, S.-M. Luo, H.-Y. Sun, X.-X. Liu, Z.-B. Wie, Syntheses and characterization of elpasolite-type ammonium alkali metal hexafluorometallates(III), J. Solid State Chem. 181 (2008) 1723–1730, https://doi.org/10.1016/j.jssc.2008.03.017.

[11] M.V. Gorev, I.N. Flerov, A. Tressaud, E.V. Bogdanov, A.V. Kartashev, O. A. Bayukov, E.V. Eremin, A.S. Krylov, Heat capacity and magnetic properties of fluoride $CsFe^{2+}Fe^{3+}F_6$ with defect pyrochlore structure, J. Solid State Chem. 237 (2016) 330–335, https://doi.org/10.1016/j.jssc.2016.02.045.

[12] M.V. Gorev, I.N. Flerov, A. Tressaud, M.S. Molokeev, A.V. Kartashev, E. I. Pogoreltsev, O.A. Bayukov, Phase transitions in fluoride KFe_2F_6 with tetragonal tungsten bronze structure, J. Fluorine Chem. 168 (2014) 204–211, https://doi.org/10.1016/j.jfluchem.2014.09.031.

[13] J.F. Scott, R. Blinc, Multiferroic magnetoelectric fluorides: why are there so many magnetic ferroelectrics? J. Phys. Condens. Matter 23 (2011), 113202 https://doi.org/10.1088/0953-8984/23/11/113202.

[14] D. Paus, R. Hoppe, Zum magnetischen Verhalten von $CsAgScF_6$, $CsCuInF_6$, $CsCuGaF_6$ sowie $CsCu_{1-x}Zn_xGaF_6$, Z. Anorg. Allg. Chem. 426 (1976) 83–94.

[15] S.C. Abrahams, J. Ravez, Dielectric and related properties of fluorine-octahedra ferroelectrics, Ferroelectrics 135 (1992) 21–37, https://doi.org/10.1080/00150199208230010.

[16] S.C. Abrahams, J. Albertsson, C. Svensson, J. Ravez, Structure of $Pb_5Cr_3F_{19}$ at 295 K, polarization reversal and the 595 K phase transition, Acta Cryst. B46 (1990) 497–502, https://doi.org/10.1107/S0108768190004256.

[17] J. Ravez, The inorganic fluoride and oxyfluoride ferroelectrics, J. Phys. III EDP Sci. 7 (1997) 1129–1144, https://doi.org/10.1051/jp3:1997175.

[18] J. Ravez, Ferroelectricity in solid state chemistry, C.R. Acad. Sci. Paris Ser. IIC Chim. Chem. 3 (2000) 267–283, https://doi.org/10.1016/S1387-1609(00)00127-4.

[19] M.R. Bauer, D.L. Pugmire, B.L. Paulsen, R.J. Christie, D.J. Arbogast, C.S. Gallagher, W.V. Raveane, R.M. Nielson, C.R. Ross II, P. Photinos, S.C. Abrahams, Aminoguanidinium hexafluorozirconate: a new ferroelectric, J. Appl. Crystallogr. 34 (2001) 47–54, https://doi.org/10.1107/S0021889800015508.

[20] M. Boča, A. Rakhmatullin, J. Mlynáriková, E. Hadzimová, Z. Vasková, M. Mičušík, Differences in XPS and solid state NMR spectral data and thermo-chemical properties of isostructural compounds in the series $KTaF_6$, K_2TaF_7 and K_3TaF_8 and $KNbF_6$, K_2NbF_7 and K_3NbF_8, Dalton Trans. 44 (2015) 17106–17117, https://doi.org/10.1039/C5DT02560E.

[21] A. Rakhmatullin, M. Boča, J. Mlynáriková, E. Hadzimová, Z. Vasková, I.B. Polovov, M. Mičušík, Solid state NMR and XPS of ternary fluorido-zirconates of various coordination modes, J. Fluorine Chem. 208 (2018) 24–35, https://doi.org/10.1016/j.jfluchem.2018.01.010.

[22] G.C. Hampson, L. Pauling, The structure of ammonium heptafluozirconate and potassium heptafluozirconate and the configuration of the heptafluozirconate group, J. Am. Chem. Soc. 60 (1938) 2702–2707.

[23] E.C. Reynhardt, J.C. Pratt, A. Watton, H.E. Petch, NMR study of molecular motions and disorder in K_3ZrF_7 and K_2TaF_7, J. Phys. C. Solid State Phys. 14 (1981) 4701–4715, https://doi.org/10.1088/0022-3719/14/31/017.

[24] M.T. Dova, M.C. Caracoche, A.M. Rodriguez, J.A. Martinez, P.C. Rivas, A.R. Lopez Garcia, Time-differential perturbed-angular-correlation study of phase transitions and molecular motions in $K_3(Hf,Zr)F_7$, Phys. Rev. B40 (1989) 11258–11263, https://doi.org/10.1103/PhysRevB.40.11258.

[25] R.L. Davidovich, D.V. Marinin, V. Stavila, K.H. Whitmire, Stereochemistry of fluoride and mixed-ligand fluoride complexes of zirconium and hafnium, Coord. Chem. Rev. 257 (2013) 3074–3088, https://doi.org/10.1016/j.ccr.2013.06.016.

[26] V.D. Fokina, M.V. Gorev, E.V. Bogdanov, E.I. Pogoreltsev, I.N. Flerov, N. M. Laptash, Thermal properties and phase transitions in $(NH_4)_3ZrF_7$, J. Fluorine Chem. 154 (2013) 1–6, https://doi.org/10.1016/j.jfluchem.2013.07.001.

[27] E. Pogoreltsev, E. Bogdanov, S. Melnikova, I. Flerov, N. Laptash, $(NH_4)_3HfF_7$: crystallooptical and calorimetric studies of a number of successive phase transitions, J. Fluorine Chem. 204 (2017) 45–49, https://doi.org/10.1016/j.jfluchem.2017.10.004.

[28] A.S. Krylov, S.N. Krylova, N.M. Laptash, A.N. Vtyurin, Raman scattering study of temperature induced phase transitions in crystalline ammonium heptafluorozirconate, $(NH_4)_3ZrF_7$, Vibrat. Spect. 62 (2012) 258–263, https://doi.org/10.1016/j.vibspec.2012.07.003.

[29] A.A. Udovenko, N.M. Laptash, Orientational disorder in crystal structures of $(NH_4)_3ZrF_7$ and $(NH_4)_3NbOF_6$, J. Struct. Chem. 49 (2008) 482–488, https://doi.org/10.1007/s10947-008-0066-8.

[30] A.A. Udovenko, A.A. Karabtsov, N.M. Laptash, Crystallographic features of ammonium fluoroelpasolites: dynamic orientational disorder in crystals of $(NH_4)_3HfF_7$ and $(NH_4)_3Ti(O_2)F_5$, Acta Cryst. B73 (2017) 1–9, https://doi.org/10.1107/S2052520616017534.

[31] E.I. Pogoreltsev, S.V. Mel'nikova, M.S. Molokeev, I.N. Flerov, N.M. Laptash, Structure, thermal and optical properties of elpasolite-like $(NH_4)_2KZrF_7$, J. Solid State Chem. 277 (2019) 376–380, https://doi.org/10.1016/j.jssc.2019.06.013.

[32] M.V. Gorev, A.V. Kartashev, E.V. Bogdanov, I.N. Flerov, N.M. Laptash, Calorimetric, dilatometric and DTA under pressure studies of the phase transitions in elpasolite $(NH_4)_2KZrF_7$, J. Fluorine Chem. 235 (2020), 109523, https://doi.org/10.1016/j.jfluchem.2020.109523.

[33] V.P. Tarasov, Y.A. Buslaev, Molecular motion and configuration of $ZrF_7^{\ 3-}$, J Struct. Chem. 10 (1970) 816–818, https://doi.org/10.1007/BF00743976.

[34] Yu.A. Buslaev, V.I. Pakhomov, V.P. Tarasov, V.N. Zege, F^{19} spin–lattice relaxation and X-ray study of phase transition in Solid K_3ZrF_7 and $(NH_4)_3ZrF_7$, Phys. Status Solidi (b) 44 (1971) K13–K15, https://doi.org/10.1002/pssb.2220440150.

[35] I.N. Flerov, M.V. Gorev, A.V. Kartashev, E.I. Pogoreltsev, N.M. Laptash, Thermodynamic properties and barocaloric effect in fluoride K_2TaF_7, J. Mater. Sci. 54 (2019) 14287–14295, https://doi.org/10.1007/s10853-019-03924-8.

[36] A.V. Kartashev, I.N. Flerov, N.V. Volkov, K.A. Sablina, Adiabatic calorimetric study of the intense magnetocaloric effect and the heat capacity of $(La_{0.4}Eu_{0.6})_{0.7}Pb_{0.3}MnO_3$, Phys. Solid State 50 (2008) 2115–2120, https://doi.org/10.1134/S1063783408110188.

[37] Bruker AXS TOPAS V4: General Profile and Structure Analysis Software for Powder Diffraction Data, 2008. Users Manual, Bruker AXS.

[38] B.J. Campbell, H.T. Stokes, D.E. Tanner, D.M. Hatch, ISODISPLACE: a web-based tool for exploring structural distortions, J. Appl. Crystallogr. 39 (2006) 607–614, https://doi.org/10.1107/S0021889806014075.

[39] O.V. Kovalev, Representations of the Crystallographic Space Groups: Irreducible Representations, Induced Representations, and Corepresentations, Gordon and Breach Science, 1993.

[40] S.C. Miller, W.F. Love, Tables of Irreducible Representations of Space Groups and Co-Representations of Magnetic Space Groups, Pruett Press, 1967.

[41] V.G. Vaks, Vvedenie v mikroscopicheskuyu teoriyu cegnetoelektrikov, Nauka, Moscow, 1973 (in Russian).

[42] I.N. Flerov, M.V. Gorev, Entropy and mechanism of phase transitions in elpasolites, Phys. Solid State 43 (2001) 127–136, https://doi.org/10.1134/1.1340198.

[43] I.P. Makarova, S.V. Misyul, L.A. Muradyan, A.F. Bovina, V.I. Simonov, K. S. Aleksandrov, Anharmonic thermal atomic vibrations in the cubic phase of $Cs_2NaNdCl_6$ single crystals, Phys. Stat. Sol. (b) 121 (1984) 481–486, https://doi.org/10.1002/pssb.2221210205.

[44] A.A. Shevyurev, L.D. Muradjan, V.E. Zavodnik, K.S. Aleksandrov, V.I. Simonov, Thermal vibrations of atoms in cubic phase of $KMnF_3$ at 198 and 293 K, Kristallografiya 25 (1980) 555–559.